Bull. Mater. Sci. (2023) 46:91
https://doi.org/10.1007/s12034-023-02920-8

Preliminary results on the characterization of ZnS and ZnS:La nanophosphors synthetized by chemical route

Y RODRÍGUEZ-LAZCANO[1], E BARRIOS-SALGADO[1,*], V CORRECHER[2], J P PÉREZ-OROZCO[3], P ALTUZAR[4] and J CAMPOS[4]

[1]Universidad Autónoma de Nayarit, Unidad Académica de Ciencias Básicas e Ingenierías, Ciudad de la Cultura "Amado Nervo" S/N, C. P. 63155 Tepic, Mexico
[2]CIEMAT, 28040 Madrid, Spain
[3]Departamento de Ingeniería Química y Bioquímica,, Instituto Tecnológico de Zacatepec, Tecnológico Nacional de México, Calzada Tecnológico # 27, Col. Centro., C. P. 62780 Mexico City, Mexico
[4]Instituto de Energías Renovables, Universidad Nacional Autónoma de México, C.P. 62580 Temixco, Morelos, Mexico
*Author for correspondence (enue.barrios@uan.edu.mx)

MS received 26 September 2022; accepted 21 December 2022

Abstract. ZnS, a semiconductor material with a bandgap in the range of 3.6–3.8 eV, can be employed as a scintillator. We herein report on the preliminary results obtained from the thermoluminescence (TL) emission of ZnS and ZnS:La nanophosphors synthesized by chemical route. The samples were characterized by X-ray diffraction, scanning electron microscopy and TL. ZnS samples show a TL maximum centred at 87°C, while the ZnS:La sample shows two groups of components appearing between 70–160°C and 190–330°C. The dose–response displays a good linearity in the range of 10–17 Gy.

Keywords. ZnS; ZnS:La; nanophosphors; thermoluminescence; chemical synthesis.

1. Introduction

ZnS doped with rare-earth (RE) elements or transition-metal can be used to develop phosphor materials due to their luminescence properties. The optical properties of La-doped ZnS nanocrystalline films have been reported [1, 2]. Also, Eu^{3+} doped ZnS nanocrystals have shown high luminescence efficiency [3]. Few studies have been done on the effects of RE-doping on the properties of the RE-doped ZnS. Zinc sulphide crystals show thermoluminescence (TL) and photoluminescence (PL) properties [4]. Many studies have been performed on the TL properties of pure and doped ZnS as powder obtained below RT [5–7]. Also, the TL of ZnS:Cu [8–10] and ZnS:Mn [11] nanophosphors have been reported. The luminescent properties of ZnS nanoparticles doped with various metallic ions (Ag^{+}, Cu^{2+}, Ce^{3+} and Sn^{4+}) have been studied [12]. The effects of deposition condition and heat treatment on the TL properties of ZnS thin films deposited by spray pyrolysis have been studied [10, 13]. Mustafa *et al* show the characterization of ZnS:Cu thin films, where copper ions can create luminescent centres by replacing either substitutionally or interstitially the zinc ions in the ZnS thin film [14]. Strong photoluminescent and cathodoluminescent emissions were observed in ZnS:Cu, Al phosphor powder prepared by a chemical solution method, which was attributed to the radiative transition at copper sites [15]. TL is the emission of light from a semiconductor or insulator when the sample is heated after being irradiated by X-rays, gamma rays, a beam of electrons, cosmic rays, etc. During heating, the TL signal is recorded as a function of temperature or wavelength. The luminescent intensity and the shape of this glow curve are functions of the radiation absorbed dose and heating rate. Luminescence phenomena depend directly on the crystalline phase. Accordingly, slight variations in the lattice structure due to the presence of impurities, substituted ions, inclusions or surface defects in ppm concentrations produce changes in the wavelength position and intensity of the emission spectra. The main aim of this research is to study the effects of La incorporation on the structural, compositional and TL properties of ZnS nanophosphors synthesized by chemical route.

2. Experimental

ZnS nanophosphors were synthesized by means of the chemical solution route following the methodology previously reported by Nair *et al* [16]. It consists of a mixture of 2.5 ml of $ZnSO_4$ 1M, 2.7 ml of $(HOCH_2CH_2)_3N$ 50%, 2.2 ml of NH_4OH/NH_4Cl (pH 10) buffer solution, 1 ml of C_2H_5NS 1M and distilled water that has been stirred for

Published online: 28 April 2023

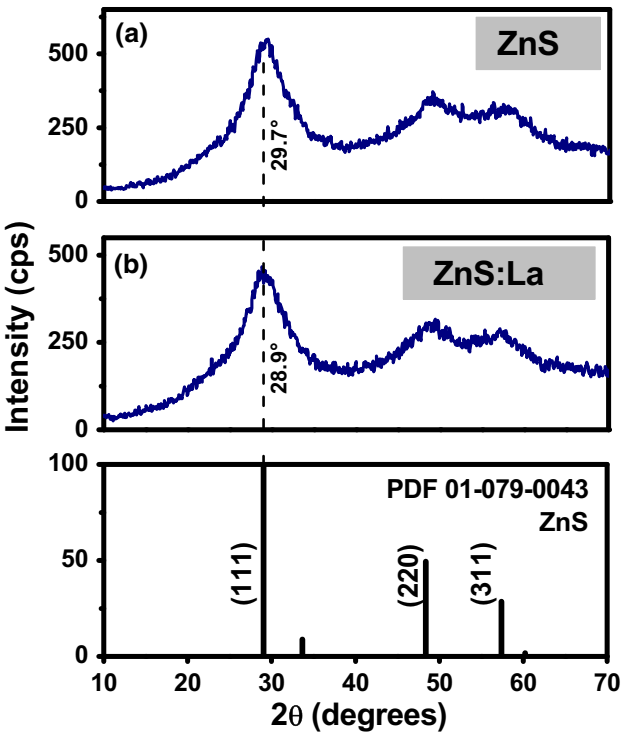

Figure 1. XRD patterns of (**a**) ZnS and (**b**) ZnS:La.

Table 1. Structural parameters calculated from XRD data.

Sample	2θ (deg.)	FWHM (deg.)	Particle size (nm)	Inter-planar spacing (Å)	Lattice constant (Å)
ZnS	29.7329	6.5484	1.31	3.0503	5.2765
ZnS-La	28.9393	9.2718	0.92	3.0827	5.3318

12 h at RT. After that, the solution was decanted, and the powder was dried in laboratory conditions to avoid potential phase transitions. The La-doped sample (0.2% of La) has been similarly prepared by adding lanthanum oxide (99.9%) to the ZnS chemical solution under constant stirring of 400 rpm. Both ZnS and ZnS:La (0.2%) samples were characterized using X-ray diffraction (XRD), where the patterns were recorded on a Rigaku Ultima IV diffractometer with monochromatized Cu K_α radiation ($\lambda = 1.5406$ Å) and incidence angle of 1.0° with the sample plane. The chemical composition was studied in an Oxford X-act energy dispersive X-ray spectrum (EDX) analyzer attached to a Hitachi-SEM SU1510. TL measurements were carried out using an automated Risø TL system model TL DA-12 [17], this reader is provided with an EMI 9635 QA photomultiplier, and the emission was observed through a blue filter (a FIB002 of the Melles-Griot Company) where the wavelength is peaked at 320–480 nm; FWHM is 80 ± 16 nm and

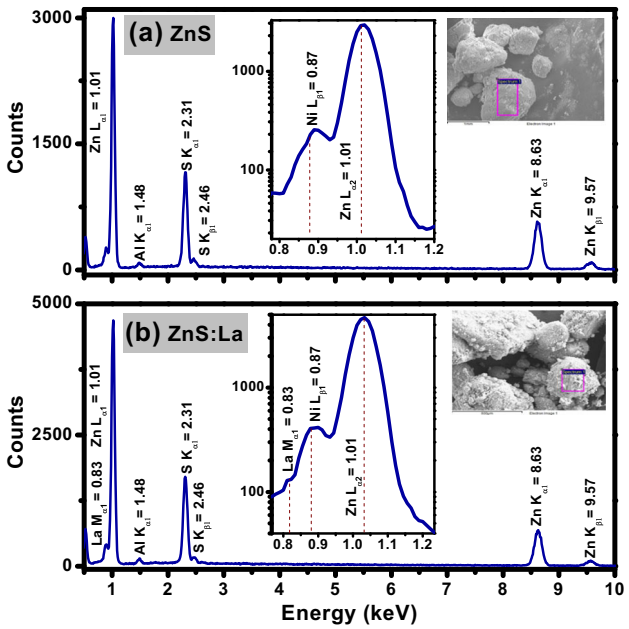

Figure 2. EDX spectra and SEM micrographs of (**a**) ZnS and (**b**) ZnS:La.

peak transmittance (minimum) is 60%. It is also provided with a $^{90}Sr/^{90}Y$ β-source with a dose rate of 0.010 Gy s^{-1} calibrated against a ^{60}Co photon source in a secondary standards laboratory [18]. All the TL measurements were performed using a linear heating rate of 5°C s^{-1} from RT up to 400°C in a N_2 atmosphere. The incandescent background was subtracted from the TL data.

3. Results and discussion

Figure 1 displays the XRD patterns of ZnS and ZnS:La. XRD patterns present diffraction peaks at 29.06°, 49.37° and 57.42°, which correspond to the (111), (220) and (311) Miller planes of cubic structure (Sphalerite) ZnS (PDF 01-079-0043), respectively. No significant differences are observed for the samples with and without lanthanum. XRD patterns of ZnS:La nanophosphors show no peaks from La_2O_3 or La, demonstrating only the formation of the ZnS crystalline phase. Additionally, slight shift to a lower angle is observed for the doped sample, which may be because the atomic radius of La (1.032 Å) is larger than Zn (0.74 Å) ionic radius. Hence, the incorporation of La ions is produced due to the replacement of Zn^{2+} ions with La^{3+} ions [12, 19]. The software of the XRD equipment calculated the particle size of the samples and the inter-planar spacing for the (111) plane. The particle size decreases slightly for La-doped ZnS, probably due to the creation of new nucleating centres from the dopant atoms in the ZnS host. The lattice constant, a, was determined using the formula $a = d\sqrt{h^2 + k^2 + l^2}$ [20]. Regarding the La-doped sample, a slight increase in the lattice constant is expected,

Table 2. Chemical composition of pure and La-doped ZnS.

Sample	Atomic %		
	Zn	S	La
ZnS	60.66	39.34	—
ZnS-La	56.27	43.56	0.17

assuming the incorporation of La into the ZnS matrix. These results are shown in table 1.

Figure 2 shows the EDX spectra with their corresponding scanning electron microscopy micrographs for ZnS and ZnS:La samples. The characteristic peaks of Zn-$L_{\alpha 1}$ at 1.01 eV, Zn-$K_{\alpha 1}$ at 8.63 eV, Zn-$K_{\beta 1}$ at 9.57 eV, S-$K_{\alpha 1}$ at 2.31 eV and S-$K_{\beta 1}$ at 2.46 eV are clearly identified, along with Al-$K_{\alpha 1}$ at 1.48 keV arising from the aliquots. A zoom in the interval of 0.7 and 1.2 eV shows a small peak at 0.83 eV that corresponds to La-$M_{\alpha 1}$ (inset of figure 2b). In the same interval, a peak associated with Ni was identified, coming from the aliquot. Also, as can be seen in table 2, the measured percentage of La is close to that incorporated in the starting solution, i.e., 0.2%. The decrease in the atomic percent of zinc and the increase in the atomic percent of sulphur can be attributed to the incorporation of La in the zinc sites of the ZnS matrix.

The TL glow curves of ZnS and ZnS:La irradiated at 10, 12, 15 and 17 Gy are displayed in figure 3. These results indicate that the impurification with La has strongly affected the TL behaviour. TL emission for ZnS sample shows a maximum at 87°C. However, ZnS:La sample shows two groups of components appearing between 70–160 and 190–330°C. These peaks can be attributed to the traps generated by the incorporation of La in the ZnS matrix at the zinc sites. TL intensity is proportional to the concentration of thermally released charges, where the thermally released charges are retrapped, at least once before the recombination process. TL signal is influenced by the dopant or background impurities. The presence of La in the ZnS samples would be explained in terms of Zn vacancy (VZn)-La defects (VZn-La), where these defects capture free electrons generated after irradiation and act as electron traps. Additionally, oxygen impurities that are adsorbed at the grain boundaries or ZnS surface act as luminescent centres in both doped and undoped ZnS [21–23]. Oxygen is considered as a background impurity coming from the synthesis process. The effect of doping ZnS with La create new traps within the material that were absent in undoped ZnS powder. In addition, hydroxyl (OH) groups adsorbed to Zn or La produces luminescence signal [24]. On the other hand, metal trace impurities coming from the raw contribute to TL emission [25].

The dose dependence of the blue TL emission from ZnS and ZnS:La nanophosphors were studied in the range of 10 to 17 Gy. As seen in figure 4, the evolution of the whole area of the induced TL peaks with the dose shows linear fitting in both cases. Values of the regression coefficient of

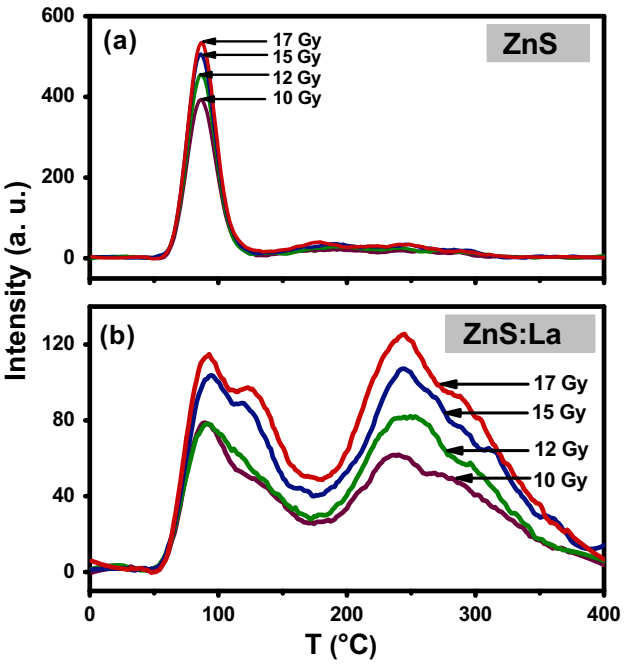

Figure 3. Glow curves of (**a**) ZnS and (**b**) ZnS:La irradiated at 10, 12, 15 and 17 Gy.

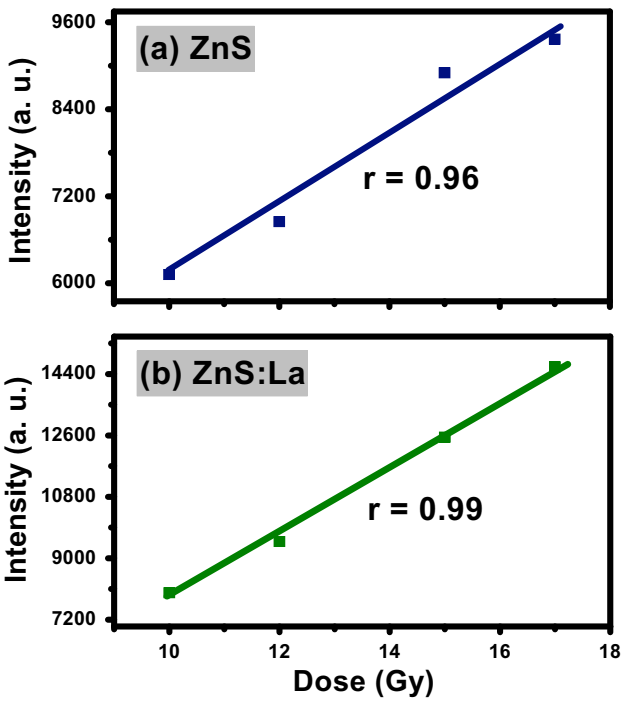

Figure 4. Dose dependence of the TL glow curve in a range of 10–17 Gy of (**a**) ZnS (area of the glow curve in a range of 50–130°C) and (**b**) ZnS:La (area of the glow curve in a range of 50–350°C).

fitting, r, were 0.96 and 0.99 for ZnS and ZnS:La, respectively. The dose–response can be fitted to an equation of the sort $y = y_0 + bx$, where y corresponds to the intensity of the TL signal, x is the given dose and y_0 is a coefficient of the equation. The area of the glow curve was taken in a range of 50–130 and 50–350°C for ZnS and ZnS:La, respectively. In the studied range of dose, no saturation has been detected.

4. Conclusions

The radiation effect on the 400 nm TL emission shows that ZnS and ZnS:La nanophosphors are sensitive to radiation and possesses dose linearity in the range of 10–17 Gy. The TL peaks, attributed to the traps generated by the incorporation of La in the ZnS matrix at the zinc sites, induce Zn vacancy (VZn)-La defects (VZn-La), that will capture free electrons generated after irradiation and act as electron traps. XRD measurements confirm the formation of only the ZnS crystalline phase. XRD and EDX results suggest the incorporation of lanthanum in the zinc sites of the ZnS matrix.

Acknowledgement

We appreciate Yareli Colin Garcia's assistance. We acknowledge the financial support of Patronato UAN through projects 'Impulso a la Investigación' and CeMIE-Sol project 35. We thank IER-UNAM through CONACYT-LIFYCS 123122 for infrastructure support. One of us (YRL) also acknowledge the financial support from PFCE-SEP-2021.

References

[1] Moustafa M, El-Barbary G, El Refaey D and El-Tantawy F 2018 *Optik* **168** 764
[2] Hai-Qing X, Yuan C, Wei-Qing H, Gui-Fang H, Ping P, Li P *et al* 2011 *Chin. Phys. Lett.* **28** 27806
[3] Qu S, Zhou W, Liu F, Chen N, Wang Z, Pan H *et al* 2002 *Appl. Phys. Lett.* **80** 3605
[4] Randall J and Wilkins M 1945 *Proc. R Soc. A* **184** 366
[5] Morton C, Forsythe E, Sun S, Wood M, Ervin M and Kirchner K 2001 *Appl. Phys. Lett.* **78** 1400
[6] Villarreal-Barajas J, Escobar-Alarcón L, González P, Camps E and Barboza-Flores M 2002 *Radiat. Meas.* **35** 355
[7] Escobar-Alarcón L, Villagran E, Camps E, Romero S, Villarreal-Barajas J and González P 2003 *Thin Solid Films* **433** 126
[8] Tiwari A, Khan S, Kher R, Dhoble S and Mehta M 2011 *J. Lumin.* **131** 2202
[9] Yazici A, Oztas M and Bedır M 2007 *Opt. Mater.* **29** 1091
[10] Yazici A, Oztas M, Kafadar V, Bedir M and Toktamıs H 2007 *J. Lumin.* **124** 58
[11] Sharma R, Bisen D, Dhoble S, Brahm N and Chandra B 2011 *J. Lumin.* **131** 2089
[12] Yang H, Huang C, Su X and Tang A 2005 *J. Alloys Compd.* **402** 274
[13] Yazici A, Oztas M and Bedır M 2003 *J. Lumin.* **104** 115
[14] Mustafa O, Metin B, Necmeddin Y, Vural K and Huseyin T 2006 *Physica B* **381** 40
[15] Qi Lai, Burtrand I, Kim M, Jang E and Choe Y. 2003 *J. Lumin.* **104** 261
[16] Nair P, Barrios-Salgado E, Capistran J, María R, Nair S and Zingaro R 2010 *J. Electrochem. Soc.* **157** D528
[17] Bøtter-Jensen L and Duller G 1992 *Nucl. Tracks Radiat. Meas.* **20** 549
[18] Correcher V, Molina D and Garcia-Guinea J 2003 *Rev. Mex. Fis.* **49** 235
[19] Chen Y, Huang G, Huang W, Zou B and Pan A 2012 *Appl. Phys. A* **108** 895
[20] Abbas M, Shehab A, Hassan N and Al-Samurae A 2011 *Thin Solid Films* **519** 4917
[21] Bube R H 1960 *Photoconductivity of solids* (New York: Wiley)
[22] Wu C and Bube R 1974 *J. Appl. Phys.* **45** 648
[23] Igarashi T, Kusunoki T, Ohno K, Isobe T and Senna M 2002 *Mater. Res. Bull.* **37** 533
[24] Garcia-Guinea J, Garrido F, Lopez-Arce P, Correcher V and de la Figuera J 2017 *J. Lumin.* **190** 128
[25] Rodríguez-Lazcano Y, Correcher V and Garcia-Guinea J 2012 *Radiat. Phys. Chem.* **81** 126